Received: 7 January 2022 | Accepted: 27 April 2022

DOI: 10.1111/2041-210X.13903

Methods in Ecology and Evolution BRITISH ECOLOGICAL SOCIETY

RESEARCH ARTICLE

# Stable isotope fingerprinting traces essential amino acid assimilation and multichannel feeding in a vertebrate consumer

**Philip J. Manlick** | **Seth D. Newsome**

Department of Biology, University of New Mexico, Albuquerque, NM, USA

**Correspondence**
Philip J. Manlick
Email: pmanlick@gmail.com

**Funding information**
Division of Biological Infrastructure, Grant/Award Number: DBI- 2010712; Division of Integrative Organismal Systems, Grant/Award Number: IOS-1755402

**Handling Editor:** Clive Trueman

## Abstract

1. Animals often consume resources from multiple energy channels, thereby connecting food webs and driving trophic structure. Such 'multichannel feeding' can dictate ecosystem function and stability, but tools to quantify this process are lacking. Stable isotope 'fingerprints' are unique patterns in essential amino acid (EAA) $\delta^{13}C$ values that vary consistently between energy channels like primary production and detritus, and they have emerged as a tool to trace energy flow in wild systems. Because animals cannot synthesize EAAs de novo and must acquire them from dietary proteins, ecologists often assume $\delta^{13}C$ fingerprints travel through food webs unaltered. Numerous studies have used this approach to quantify energy flow and multichannel feeding in animals, but $\delta^{13}C$ fingerprinting has never been experimentally tested in a vertebrate consumer.
2. We tested the efficacy of $\delta^{13}C$ fingerprinting using captive deer mice *Peromyscus maniculatus* raised on diets containing bacterial, fungal and plant protein, as well as a combination of all three sources. We measured the transfer of $\delta^{13}C$ fingerprints from diet to consumer liver, muscle and bone collagen, and we used linear discriminant analysis (LDA) and isotopic mixing models to estimate dietary proportions compared to known contributions. Lastly, we tested the use of published $\delta^{13}C$ source fingerprints previously used to estimate energy flow and multichannel feeding by consumers.
3. We found that EAA $\delta^{13}C$ values exhibit significant isotopic (i.e. trophic) fractionation between consumer tissues and diets. Nevertheless, LDA revealed that $\delta^{13}C$ fingerprints are consistently routed and assimilated into consumer tissues, regardless of isotopic incorporation rate. Isotopic mixing models accurately estimated the proportional diets of consumers, but all models overestimated plant-based protein contributions, likely due to the digestive efficiencies of protein sources. Lastly, we found that $\delta^{13}C$ source fingerprints from published literature can lead to erroneous diet reconstruction.
4. We show that $\delta^{13}C$ fingerprints accurately measure energy flow to vertebrate consumers across tissues with different isotopic incorporation rates, thereby enabling the estimation of multichannel feeding at various temporal scales. Our findings illustrate the power of $\delta^{13}C$ fingerprinting for quantifying food web

dynamics, but also reveal that careful selection of dietary source data is critical to the accuracy of this emerging technique.

**KEYWORDS**
biogeochemistry, brown food web, compound-specific stable isotope analysis, foraging, green food web, mammal, nutrition, trophic ecology

## 1 | INTRODUCTION

Mapping energy flow and food web structure is one of the oldest and most pervasive questions in ecology (Lindeman, 1942). Natural food webs are defined by countless reticulate connections between consumers and resources that link energy channels and regulate ecosystem functions (Polis, 1991; Polis & Strong, 1996; Thompson et al., 2012). Classically, food webs were grouped into two independent energy channels—'green' grazer chains supported by primary production or 'brown' detrital chains fuelled by decomposition (Polis & Strong, 1996). However, the mixing of green and brown energy channels is increasingly recognized as a critical component of natural ecosystems that can stabilize food webs (Wolkovich et al., 2014), regulate ecosystem function (Zou et al., 2016) and dictate trophic structure (Steffan et al., 2017).

Consumers play a central role in connecting food webs by foraging on resources from both green and brown energy channels (Wolkovich et al., 2014). Such 'multichannel feeding' is exceedingly common and has been documented in taxa ranging from arthropods (Perkins et al., 2017) to fishes (Elliott Smith et al., 2020) to mammals (Pauli et al., 2019). Quantifying multichannel feeding by consumers is challenging, however, and ecologists have historically relied on visual observations and gut content analysis, which can be subjective or provide biased estimates of energy flow (Symondson, 2002). Increasingly, labelled or natural abundance chemical tracers like stable isotopes (e.g. $\delta^{13}C$ or $\delta^{15}N$) have enabled researchers to trace energy flow through food webs and estimate multichannel feeding (Butler et al., 2008; Perkins et al., 2017). For example, bulk tissue stable isotope analysis can track the use of $C_3$ versus $C_4$ primary production (Noble et al., 2019) or benthic versus pelagic production (Vander Zanden & Vadeboncoeur, 2002). However, the processes driving bulk tissue isotope patterns in green and brown resources are many (e.g. baseline variation, metabolic processing), often resulting in ambiguous estimates of multichannel feeding (Pollierer et al., 2019; Potapov, Tiunov, & Scheu, 2019).

Stable isotope analysis of individual amino acids has emerged as a promising tool to quantify multichannel feeding and energy flow in complex systems (Larsen et al., 2013). In particular, $\delta^{13}C$ analysis of essential amino acids (EAAs) may provide an ideal tool for quantifying multichannelling because EAAs can be synthesized by 'green' photoautotrophs (e.g. plants, algae) or 'brown' decomposers (e.g. bacteria, fungi). Importantly, each of these groups synthesize EAAs using unique biosynthetic pathways that lead to distinct, multivariate patterns in $\delta^{13}C$ values—termed 'fingerprints'—that differ significantly between green and brown energy sources (Larsen et al., 2009, 2013). In contrast, animals cannot synthesize EAAs at rates sufficient to meet metabolic demands and therefore must acquire these molecules from their diets, potentially enabling the use of $\delta^{13}C$ fingerprints to trace the flow of green versus brown carbon from primary synthesizers to consumers (Harada et al., 2022). It is often assumed that $\delta^{13}C$ fingerprints travel through food webs unaltered because EAAs exhibit minimal isotopic fractionation between consumers and diet (McMahon et al., 2010, 2015), and numerous studies have used $\delta^{13}C$ fingerprints to quantify the flow of carbon to wild consumers (e.g. Fox et al., 2019; McMahon et al., 2016; Potapov, Tiunov, Scheu, Larsen, et al., 2019). However, experimental soil food webs recently uncovered considerable variation in $\delta^{13}C$ fingerprints due to trophic fractionation of EAA $\delta^{13}C$ values, leading to inaccurate estimates of energy flow (Pollierer et al., 2019). Moreover, $\delta^{13}C$ fingerprinting is currently hindered by an inconsistent application of statistical (e.g. normalization) and methodological (e.g. isotopic mixing models) approaches used to estimate proportional diet contributions, none of which have been tested rigorously in a controlled setting. These discrepancies indicate a need for controlled feeding experiments to (a) assess whether EAA $\delta^{13}C$ fingerprints are transferred unaltered from dietary protein to consumer tissues and (b) assess the efficacy of methods used to quantify this transfer (Pollierer et al., 2019; Whiteman et al., 2019).

Here, we present an experimental test of $\delta^{13}C$ fingerprinting in a vertebrate consumer using diets with known protein sources and proportions to assess the accuracy of common analytical approaches for quantifying multichannel feeding. We used captive deer mice (*Peromyscus maniculatus*; $N = 40$) raised on diets containing exclusively bacterial, fungal or plant protein, and a fourth diet using a combination of all three sources. We then assessed the routing and assimilation of $\delta^{13}C$ fingerprints from diet to three consumer tissues with varying isotopic incorporation rates, and we used a suite of bootstrapping and isotopic mixing model approaches to estimate dietary proportions compared to known contributions. Lastly, we used our controlled data to test the efficacy of two common practices: (1) the use of published $\delta^{13}C$ source fingerprints (e.g. Larsen et al., 2009, 2013) to estimate multichannel feeding in consumers and (2) statistical normalization of source data when estimating consumer diets.

## 2 | MATERIALS AND METHODS

We raised 40 weanling deer mice (*P. maniculatus*) on controlled diets using animals from a captive colony at the University of New Mexico Animal Research Facility (UNM-ARF; Albuquerque, NM, USA; Table S1).

Breeding pairs were established at UNM-ARF in 2019 from a source colony at the National Institute of Allergies and Infectious Diseases Rocky Mountain Laboratories, and all breeding individuals were fed plant-based commercial diets (Teklad Global Rodent Diets®, Envigo) ad libitum to promote offspring development. After birth, individuals were monitored for 21 days, at which point they were weaned, transitioned to commercial diets and held for a 14-day acclimation period. At 35 days, weanlings were randomly assigned to one of four experimental diet treatments (see below). All animals were housed communally by diet treatment in 18×12-inch plastic containers with wire-bottom shelves to separate faeces and minimize coprophagy. UNM-ARF maintained a constant temperature of ~22°C with a photoregimen of 12 hr days and 12 hr nights. All animal handling and husbandry was conducted under approval by the UNM Institutional Animal Care and Use Committee (19-200,801-MC, 19-200,821-B-MC).

## 2.1 | Experimental design

We raised weanling deer mice on four experimental diets with balanced macromolecular profiles including 15% (weight percent) crude protein, 45% sucrose and 5% lipids, in addition to structural carbohydrates, fortified salt and vitamins (Table 1). To assess the efficacy of $\delta^{13}C$ fingerprinting for tracing green and brown energy flow from diets to consumers, we fed mice plant, fungal, and bacterial protein sources that exhibited unique $\delta^{13}C$ fingerprints (see below). We varied protein sources across four treatments: (a) soy protein isolate ($N = 9$ mice, hereafter 'plant'; [MP Biomedicals LLC]; (b) torula yeast protein isolate ($N = 11$, hereafter 'fungi'; MP Biomedicals); (c) bacterial protein isolate ($N = 10$, hereafter 'bacteria'; Feedkind®, Calysta, Inc.); and (d) mixed protein isolates ($N = 10$, 33% each of plant, fungi, bacteria) (Table 1). Crude protein content varied by protein isolate, so structural carbohydrate content (cellulose) was adjusted per diet to achieve the target crude protein weight percentage (Table 1). Ingredients were homogenized with 4–6 L of water and stored frozen (−20°C) until provisioned. Food and water were provided ad libitum, with ~14–22 g of food provisioned daily depending on treatment. Mice were held on controlled diets for up to 184 days ($\bar{x} = 145.9$, Table S1), at which point they were euthanized via $CO_2$ asphyxiation and tissues were harvested for stable isotope analysis. This period represented an average mass gain of 9.1 g, or 34.4% of the individual's final mass. Experimental manipulations adhered to ethical guidelines outlined by the outlined by the American Society of Mammalogists (Sikes, 2016).

## 2.2 | Stable isotope analysis

We collected three tissues with known isotopic incorporation rates: liver (~20 days), skeletal muscle (quadriceps femoris; ~90 days) and bone collagen (femur; >180 days) (Dalerum & Angerbjörn, 2005; Miller et al., 2008). Prior to isotopic analysis, bone samples were demineralized in 0.5 N HCL for 24 hr at 4°C, and all tissues were soaked in 2:1 chloroform: methanol solution for 72 hr to extract lipids; fresh aliquots of solution were replaced every ~24 hr. Samples were rinsed with deionized water following each procedure and then freeze-dried for 24 hr.

For EAA $\delta^{13}C$ analysis, all tissue samples and dietary protein sources [plant ($n = 15$), bacteria ($n = 11$), fungi ($n = 10$) and mixed ($n = 12$) protein isolates] were weighed to 10–20 mg and hydrolysed in 1 ml of 6 N HCL for 20 hr at 110°C. Amino acids were then derivatized to N-trifluoroacetic acid isopropyl esters following established protocols (Silfer et al., 1991; Whiteman et al., 2019). Because the reagents used to derivatize EAAs add carbon to the amine and carboxyl groups of amino acids, measured $\delta^{13}C$ values represent a combination of carbon from the sample and the reagents (Silfer et al., 1991). To correct for this added carbon, samples were derivatized in batches alongside an in-house reference material containing a solution of pure amino acids (Sigma Aldrich) that were individually measured for $\delta^{13}C$ using a Costech 4010 elemental analyser (Costech) coupled to a Thermo Scientific Delta V isotope ratio mass spectrometer (IRMS; Thermo Fisher Scientific). This reference material was then used to correct EAA $\delta^{13}C$ values in all downstream measurements (see below; Table S2).

**TABLE 1** Macromolecular composition (weight percent) of diet treatments. All diets included 15% protein, but sources varied in crude protein content (%). Structural carbohydrates (i.e. cellulose) were adjusted to maintain protein concentrations across treatments. Footnote outlines additional compounds present in crude protein sources

| Ingredient | Macromolecule | Protein source | Crude Protein[a] | Treatment 1 | Treatment 2 | Treatment 3 | Treatment 4 |
|---|---|---|---|---|---|---|---|
| Soy Isolate | Protein | Plant | 0.92 | 0.15 | — | — | 0.05 |
| Torula Yeast | Protein | Fungi | 0.60 | — | 0.15 | — | 0.05 |
| Feedkind® | Protein | Bacteria | 0.71 | — | — | 0.15 | 0.05 |
| Sucrose | Carbohydrate | — | — | 0.45 | 0.45 | 0.45 | 0.45 |
| Cellulose | Structural Carbohydrate | — | — | 0.29 | 0.20 | 0.24 | 0.24 |
| Fortified Salt | Salt | — | — | 0.04 | 0.04 | 0.04 | 0.04 |
| Vitamin Mix | Vitamins | — | — | 0.01 | 0.01 | 0.01 | 0.01 |
| Corn Oil | Lipid | — | — | 0.05 | 0.05 | 0.05 | 0.05 |

[a]Additional weight percentages include moisture (4.1%–6.8%), ash (3.6%–7.0%), oils (0.3%–7.29%) and minerals.

Derivatized amino acids were separated and analysed via gas chromatography combustion isotope ratio mass spectrometry (GC-C-IRMS) by first injecting 1 μl of sample into a Trace 1310 gas chromatograph (Thermo Scientific) with a BPx5 column (60 m long, 0.32 mm ID, 1.0 μm film thickness; SGE Analytical Science, Ringwood, Australia). Individual amino acids were then combusted into $CO_2$ with a GC Isolink II before $\delta^{13}C$ analysis on a Thermo Scientific Delta V IRMS. All samples were injected in duplicate and bracketed with in-house reference material, which was used to correct the measured $\delta^{13}C$ values of samples following O'Brien et al. (2002). We measured $\delta^{13}C$ values for 14 amino acids (Appendix 1; Manlick & Newsome, 2022), but here we focus on six EAAs used for $\delta^{13}C$ fingerprinting: isoleucine (Ile), leucine (Leu), lysine (Lys), phenylalanine (Phe), threonine (Thr) and valine (Val). We report all isotopic data in δ-notation. We used the internationally recognized $\delta^{13}C$ standard Vienna-Pee Dee Belemnite, and results are reported as parts per mille (‰). In total, we conducted 39 GC-C-IRMS runs with 160 total reference injections ($\bar{x}$ = 4.10/run), and the mean within-run standard deviation was ≤0.48‰ for all EAAs (Table S2). All analyses were conducted at the University of New Mexico Center for Stable Isotopes.

## 2.3 | Stable isotope fingerprints

To assess the routing of EAA $\delta^{13}C$ values, we first tested for trophic fractionation using unpaired two-sample *t*-tests with a Bonferroni correction to compare the $\delta^{13}C$ values of each EAA in consumer tissues to their protein treatment. We then tested for multivariate differences between treatments in both the diets and consumers using a perMANOVA in the R package VEGAN v2.5-7 (Oksanen et al., 2013). To identify $\delta^{13}C$ fingerprints and predict the origins of EAAs in consumer tissues, we then used linear discriminant analysis (LDA) in the R package MASS v7.3-54 (Ripley et al., 2013). LDA maximizes separation of groups in multivariate space and has proved a powerful approach for distinguishing energy channels based on $\delta^{13}C$ values of EAAs (Larsen et al., 2009, 2013). We used the $\delta^{13}C$ values of all EAAs from the plant, fungi and bacteria protein sources in an LDA to first train the model, and we used leave-one-out cross-validation to assess whether sources could be assigned to their respective groups with high (>80%) classification accuracy. We then used this model to predict group membership for animal tissues. Due to variation in isotopic incorporation rates between tissues, we restricted all statistical analyses of liver, muscle and bone collagen to animals held on diets for ≥20 days, ≥50 days and ≥160 days, respectively, to ensure that tissues reached isotopic steady state with their respective diets, as quantified in previous feeding experiments (Miller et al., 2008).

## 2.4 | Proportional diet analyses

Estimating proportional contributions of diet sources to consumers via $\delta^{13}C$ fingerprints has been challenging because the established LDA approach assigns consumer tissues to a single potential source and is unable to estimate contributions from multiple sources. Accordingly, multiple approaches, including Bayesian isotopic mixing models (McMahon et al., 2016; Potapov, Tiunov, Scheu, Larsen et al., 2019) and LDA bootstrapping (Fox et al., 2019), have been employed to estimate proportional contributions of energy channels (e.g. plant, fungi, bacteria; Potapov, Tiunov, Scheu, Larsen, et al., 2019). However, none of these approaches have been tested using organisms on controlled diets. We estimated the proportional contributions of protein sources for all consumer tissues determined to be in isotopic steady state in the plant, fungi, bacteria and mixed diet treatments using four common approaches: (a) a Bayesian isotopic mixing model using $\delta^{13}C$ values from all measured EAAs and (b) a Bayesian isotopic mixing model using $\delta^{13}C$ values from the three most informative EAAs as identified by LDA loadings (i.e. coefficients); (c) a Bayesian isotopic mixing model using linear discriminant coordinates of consumers and sources; and (d) LDA bootstrapping.

First, we used all measured EAA $\delta^{13}C$ values for consumers and resources in a three-source (plant, fungi and bacteria), six-tracer (Ile, Leu, Lys, Phe, Thr and Val) isotopic mixing model implemented in the R package SIMMR v0.4.5 (Parnell & Inger, 2016). Animals from each diet treatment were categorized as a unique group, and we used a trophic discrimination factor (TDF) estimated as the difference between $\delta^{13}C$ values in consumers and diets for all treatments and amino acids (i.e. $\Delta^{13}C_{Consumer\text{-}Diet}$; Table S3). Second, we identified the three most informative EAAs as those with the largest LDA loadings and then ran a three-source, three-tracer mixing model in *simmr* using only $\delta^{13}C$ values from this subset of EAAs, but with the same TDF and group parameterization as above. While TDFs were estimated directly for this experiment, tissue- and diet-specific fractionation for EAAs is often unknown and ecologists assume negligible trophic fractionation. Therefore, we also ran both models with a TDF of zero to test the sensitivity of this parameter. Third, we ran a three-source, two-tracer mixing model in *simmr* using the first and second linear discriminant coordinates (hereafter, 'LDA coordinates') for consumers and diets generated via the isotopic fingerprinting approach outlined above. This approach also assumes direct routing of $\delta^{13}C$ fingerprints, so we applied a TDF of zero. All mixing models were run for the default 10,000 iterations with a 1,000-iteration burn-in, and model convergence was confirmed via Gelman–Rubin diagnostic values <1.05. Lastly, we estimated proportional diets using a two-step LDA bootstrap procedure (Fox et al., 2019) with 10,000 iterations of the model where dietary sources were randomly sampled (with replacement) from the EAA $\delta^{13}C$ data for each dietary protein source (i.e. plant, fungi, bacteria). This results in subtle variation in the dietary source error distributions for each iteration to which consumers are then classified, thereby providing a distribution of possible classifications, which was used to estimate the mean contribution (with 95% confidence interval) of plant, fungi and bacteria EAAs to mouse tissues (sensu Fox et al., 2019).

### 2.5 | Testing common approaches

The emergence of stable isotope fingerprinting has been facilitated by the availability of EAA $\delta^{13}C$ data from primary synthesizers first reported by Larsen et al. (2009, 2013), and these data have now been employed to putatively estimate consumer diets and multichannel feeding across aquatic, marine and terrestrial ecosystems (Arthur et al., 2014; Potapov, Tiunov, Scheu, Larsen, et al., 2019; Thorp & Bowes, 2017). However, the applicability of this data to estimate consumer foraging across systems remains uncertain (McMahon et al., 2016). To test the efficacy of this approach, we used the canonical Larsen et al. (2009, 2013) $\delta^{13}C$ EAA data for plants, fungi and bacteria in the LDA approach outlined above to first train the model, and we then predicted group classification for mouse tissues analysed in this study. We restricted this analysis to the single protein treatments (i.e. bacteria, fungi and plant) that could be assigned to a single, known protein source, and we then calculated the classification accuracy for each treatment when using the Larsen et al. (2009, 2013) data as putative sources. Similarly, many studies normalize $\delta^{13}C$ EAA data to sample means prior to multivariate analyses, but this practice is inconsistently applied across the literature and its effect on $\delta^{13}C$ fingerprints and LDA assignments has also not been tested in a controlled setting. We used our experimental data to test this approach by normalizing consumer and source $\delta^{13}C$ EAA values to the sample mean for each tissue. We then used our LDA approach as above to train the models, predict group classification for mouse tissues and calculate classification accuracy. This analysis was also restricted to the single protein treatments.

## 3 | RESULTS

### 3.1 | Multivariate analyses

We measured EAA $\delta^{13}C$ values in 39 liver samples ($N_{Bacteria}$ =10, $N_{Fungi}$ =11, $N_{Plant}$ =8, $N_{Mix}$ =10), 38 muscle samples ($N_{Bacteria}$ =10, $N_{Fungi}$ =10, $N_{Plant}$ =8, $N_{Mix}$ =10) and 30 bone collagen samples ($N_{Bacteria}$ =9, $N_{Fungi}$ =10, $N_{Plant}$ =4, $N_{Mix}$ =7). Premature mortality prevented the remaining individuals from reaching isotopic steady state with their diets and were therefore excluded from analyses. Two-sample *t*-tests revealed at least one significant difference ($p$ <0.05) in $\delta^{13}C$ values between tissue and diet among all treatments and tissues (Figure 1; Figure S1). Likewise, we observed significant differences between tissue and diet in all EAAs except Lys and Phe (Figure 1). Bone collagen $\delta^{13}C$ values exhibited the most significant differences from diet, including all EAAs in the bacteria treatment (Figure S1), suggesting it had not reached isotopic equilibrium with dietary protein. Therefore, bone collagen was excluded from all downstream analyses, and we report results from liver and muscle data only. Our perMANOVAs detected significant differences in EAA $\delta^{13}C$ values between treatments for source proteins, as well as liver and muscle tissue (all $p$ <0.001). Similarly, LDA identified consistent multivariate differences in source proteins (i.e. fingerprints, Figure 2), and leave-one-out cross-validation resulted in 100% classification accuracy for plant, fungi and bacterial

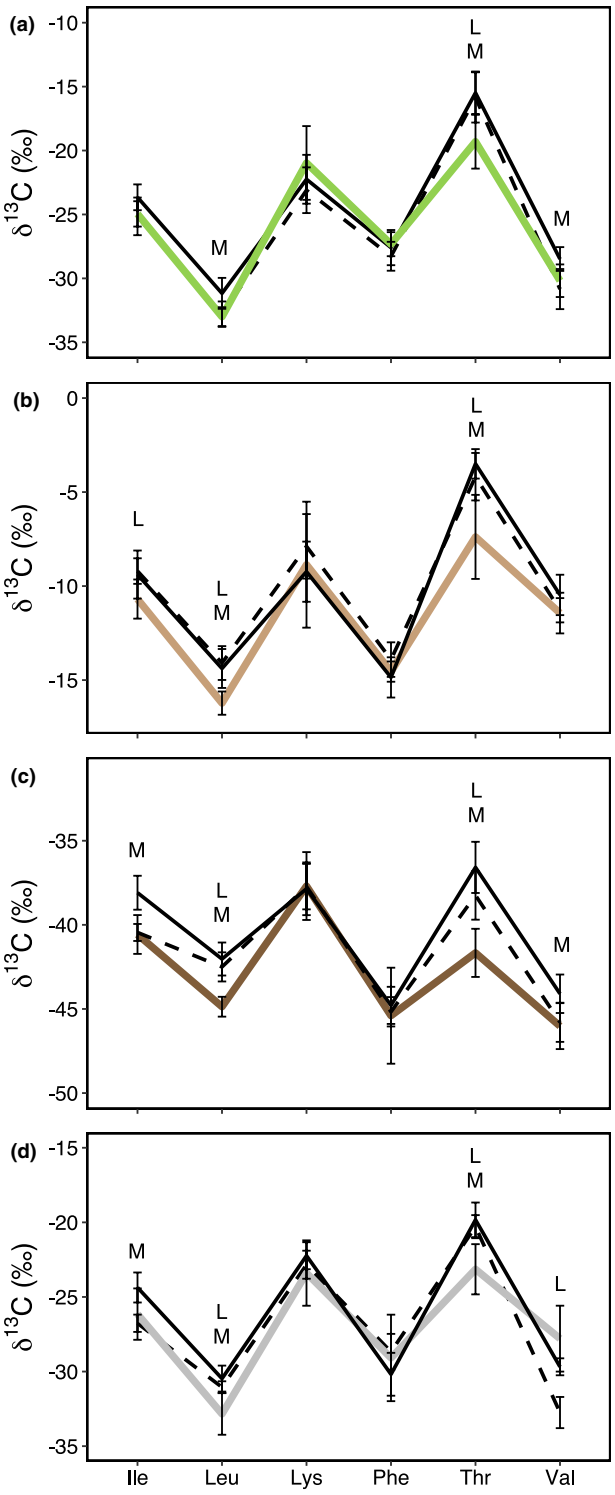


**FIGURE 1** Carbon isotope ($\delta^{13}C$) values and standard deviations (vertical lines) for essential amino acids (EAAs) from mouse tissues and diet treatments. Treatments included plant protein (a, green), fungal protein (b, light brown) and bacterial protein (c, dark brown), and an equal mix of all three (d, grey). Lines represent measured $\delta^{13}C$ values for dietary protein sources (colours), liver tissue (dashed black) and muscle tissue (solid black). Measured EAAs included isoleucine (Ile), leucine (Leu), lysine (Lys), phenylalanine (Phe), threonine (Thr) and valine (Val). Significant differences between liver (L) and muscle (M) tissues and their respective diet treatments represented by capital letters. Note the *y*-axis varies by dietary source.

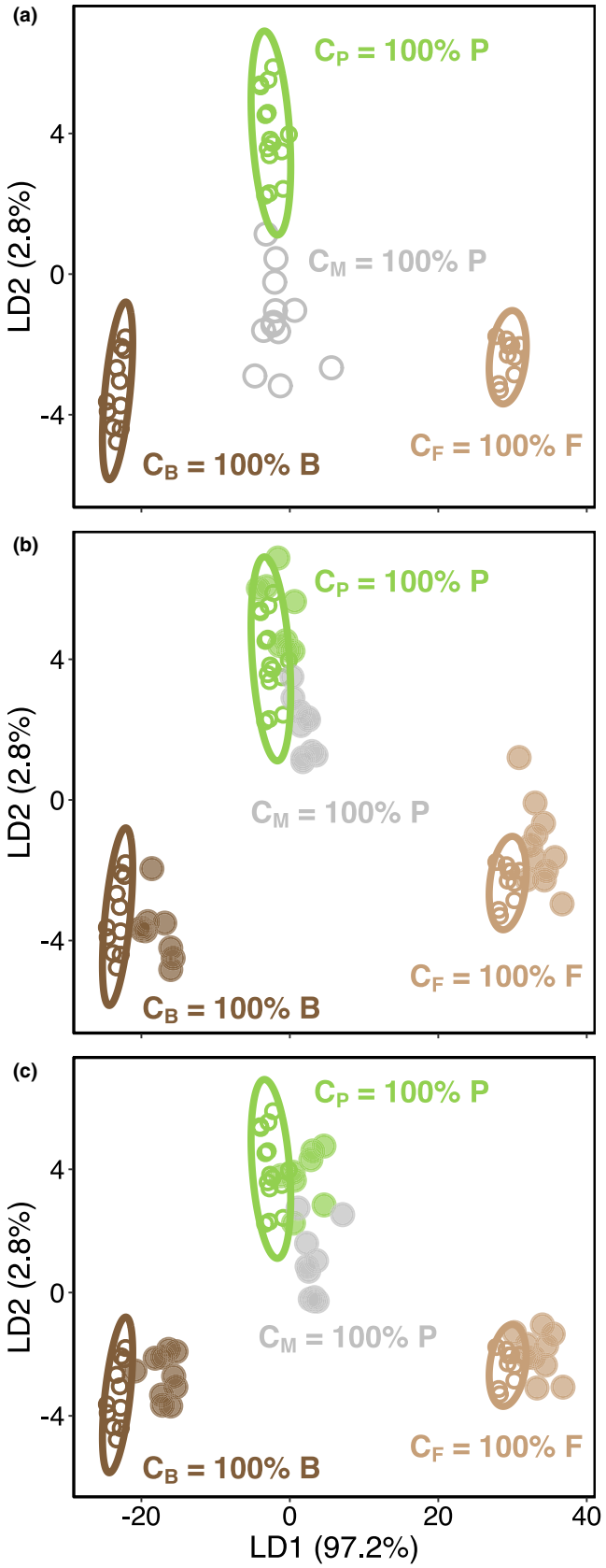


**FIGURE 2** Linear discriminant analysis (LDA) of dietary protein sources (open circles) and consumer tissues (filled circles) using $\delta^{13}C$ values from six essential amino acids: isoleucine, leucine, lysine, phenylalanine, threonine and valine. (a) Diet treatments, including plant (green), fungi (light brown), bacteria (dark brown) and mixed (grey) protein. (b) Liver tissue (filled circles) from mice in each treatment. (c) Muscle tissue (filled circles) from mice in each treatment. Classification accuracy ($C_{Treatment}$) denotes the percent of individuals assigned to plant (P), fungi (F) and bacterial (B) protein sources per treatment. Standard ellipse areas (95%) for each source represented by solid lines, and axes denote the percent of variation described by each linear discriminant (LD).

proteins. The most discriminatory EAAs (i.e. highest coefficients) were Leu, Ile and Lys (Table S4). Consumer tissues also exhibited perfect assignment, as both liver and muscle from animals on the plant, fungi and bacteria treatments exhibited 100% classification accuracy (Figure 2b,c). Mixed protein diets were visually different from pure protein diets in LDA space (Figure 2a) but classified as plant protein, as did all liver and muscle tissue from the mixed treatment animals (Figure 2b,c).

### 3.2 | Proportional diet estimates

Proportional diet estimates yielded accurate and similar results for all single protein diets using all approaches, and model results were nearly identical for liver and muscle tissue (Figure 3). Mean diet proportions from all three mixing models and the LDA bootstrap estimated 82.9%–100% bacterial protein for the bacteria treatment, 92.2%–100% fungal protein for the fungi treatment and 66.4–100% plant protein for the plant treatment (Figure 3, Tables S2–S3). In all cases, LDA bootstrapping produced higher proportional estimates with less error than mixing model-based approaches (Figure 3). The plant treatment yielded the highest variation in mean estimates between modelling approaches, as well as the highest uncertainty within models (Figure 3). The mixed diet treatment (33% of each protein) revealed greater differences among approaches, with mixing models using measured $\delta^{13}C$ EAA values exhibiting the most accurate mean diet estimates: 19.0%–55.9% for all sources (Figure 3). All approaches overestimated the mean proportional contribution of plant protein (Figure 3), with mixing models estimating 42.9%–70.2% plants and LDA bootstrapping reporting 100% plant-based protein with zero error (i.e. all 10,000 iterations of the LDA classified mixed diet consumers with plants). Models with and without EAA-specific TDFs produced comparable estimates for all diets and tissues, except when estimating proportional contributions from mixed diets using only the three most informative EAAs, in which case plant protein estimates decreased in the absence of TDFs and proportional contributions became more even (Figure S2).

### 3.3 | Common approaches

The use of published EAA $\delta^{13}C$ data for plant, fungi and bacterial protein derived from Larsen et al. (2009, 2013) yielded spurious classifications when applied to our consumers with known diets (Figure 4). Notably, mice from plant and bacterial treatments accurately classified to their respective protein sources (87.5%–100%) for both liver and muscle tissue; however, only 9.1% and 40.0% of consumers from

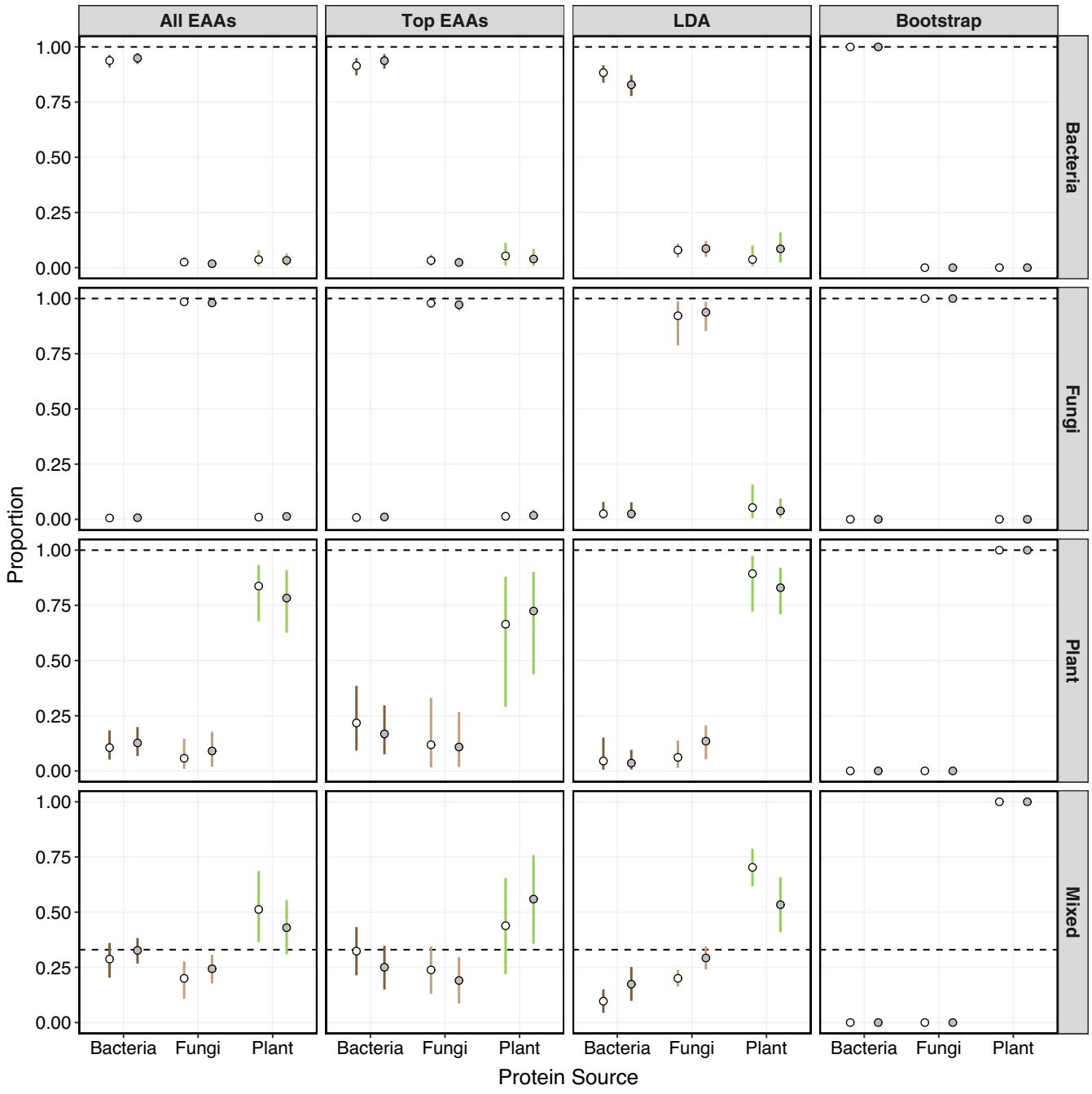


**FIGURE 3** Mean proportional diet estimates for mice in each treatment (rows) using four statistical approaches (columns): Bayesian mixing model with $\delta^{13}C$ values from all six essential amino acids (All EAAs); Bayesian mixing model with $\delta^{13}C$ values from three most informative essential amino acids as identified by linear discriminant analysis (top EAAs); Bayesian mixing model with coordinates from linear discriminant analysis (LDA) and iterative LDA bootstrapping (Bootstrap). Estimates were made for liver (white) and muscle (grey) tissue separately, and diet sources included bacteria (dark brown), fungi (light brown) and plant (green) protein. Dashed lines indicate known diet proportions for single protein diets (1) and mixed protein diets (0.33), while solid vertical lines represent 95% credible intervals for mixing model approaches and 95% confidence intervals for LDA bootstrapping. Columns 1–2 (All EAAs, Top EAAs) include tissue discrimination factors derived from this study.

the fungal protein treatment accurately classified with fungi for liver and muscle tissue, respectively (Figure 4). Statistical normalization had almost no influence on fingerprinting classifications, as only 1 of 77 normalized samples classified incorrectly compared to the 100% accuracy of non-normalized samples (Figure S3).

## 4 | DISCUSSION

Ecologists have long struggled to quantify multichannel feeding and the integration of green and brown food webs using classical approaches like stomach content analyses. We used a captive feeding

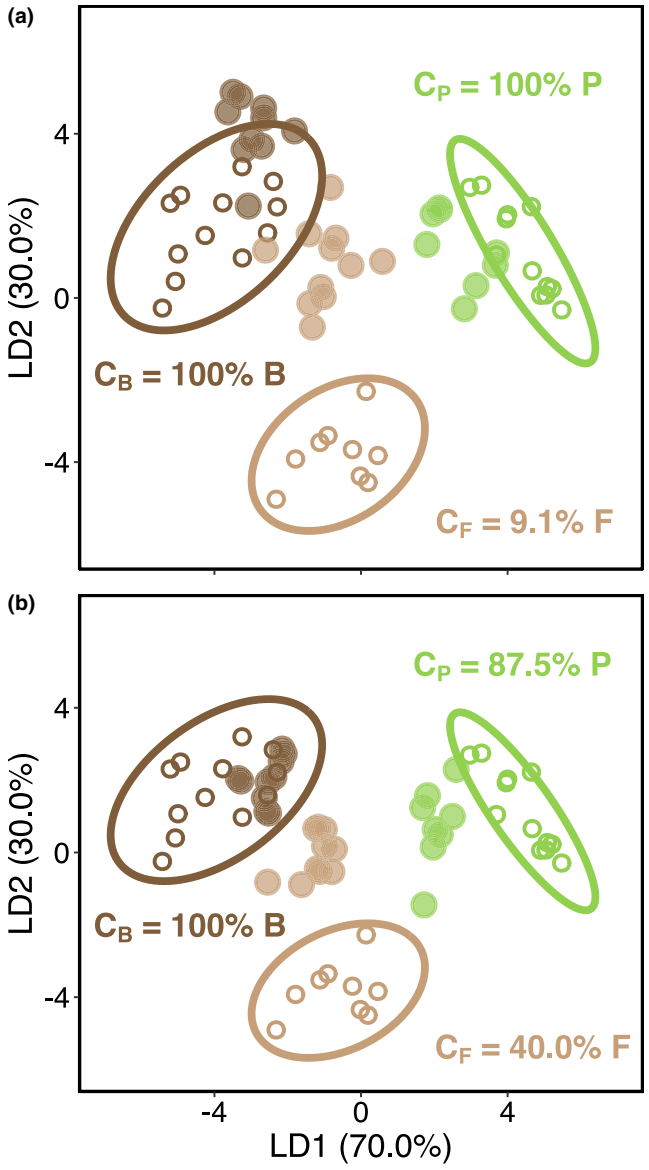


**FIGURE 4** Linear discriminant analysis (LDA) using published $\delta^{13}C$ source values for essential amino acids (isoleucine, leucine, lysine, phenylalanine, threonine and valine) reported by Larsen et al. (2009, 2013). Plant (green), fungi (light brown) and bacteria (dark brown) from Larsen et al. (2009, 2013) are denoted by open circles and mouse liver (a) and muscle (b) tissues from controlled feeding experiment are denoted by filled circles. Classification accuracy ($C_{Treatment}$) denotes the percent of individuals correctly assigned to plant (P), fungi (F) and bacterial (B) protein sources given their known dietary treatment. Standard ellipse areas (95%) for each source represented by solid lines, and axes denote percent variation described by each linear discriminant (LD).

experiment to test the efficacy of an emerging technique—$\delta^{13}C$ fingerprinting—and show that natural isotopic patterns in EAAs present in dietary protein sources are assimilated and routed into consumer tissues with minimal alteration. Moreover, we found that the isotopic routing of $\delta^{13}C$ fingerprints is consistent across consumer tissues with varying rates of isotopic incorporation (e.g. liver, muscle), thereby enabling the estimation of multichannel feeding across temporal scales. Using a series of Bayesian isotopic mixing models, we also accurately estimated the proportional contributions of green and brown protein sources (i.e. energy channels) to consumers from controlled diets for the first time. Collectively, these results demonstrate that $\delta^{13}C$ fingerprinting provides a powerful new tool to quantify multichannel feeding with unprecedented ecological resolution.

Animals cannot synthesize EAAs at rates sufficient to meet their metabolic demands, so it is often assumed that EAAs in consumer tissues are routed directly from their diets and therefore have similar $\delta^{13}C$ values to dietary protein (i.e. small TDFs; McMahon et al., 2016). Furthermore, EAA fingerprinting of consumer tissues assumes no trophic fractionation, with the expectation that the patterns in consumer EAA $\delta^{13}C$ values map perfectly with those of their dietary protein sources (Larsen et al., 2013). However, we detected consistent differences in EAA $\delta^{13}C$ values between tissue and diet, with significant trophic fractionation across tissues, diet treatments and individual amino acids (Figure 1; Table S3). Notably, we observed consistent trophic enrichment in both Leu and Thr across tissues and treatments, likely due to physiological processes. For example, Thr is a biochemical precursor to non-essential amino acids like glycine and serine, and it is possible that isotopically light Thr was preferentially catabolized to make these biomolecules, thereby leaving Thr $\delta^{13}C$ in consumer tissues enriched relative to their diets (McMahon et al., 2010; Wu, 2009). Similarly, we observed significant fractionation in Leu, Ile and Val, all branch-chained EAAs that tend to be oxidized for energy at high rates (Wu, 1998, 2009; Figure 1). These findings are consistent with recent feeding experiments showing significant trophic fractionation in EAAs (e.g. Whiteman et al., 2018), a pattern that is likely to occur when dietary protein content is high and EAAs are in excess (Whiteman et al., 2021). Our experimental diets provided 15% crude protein with amino acid proportions approximating that of mouse tissues (Figure S4; Wolf et al., 2015). *Peromyscus* species generally require 14%–30% dietary protein (McAdam & Millar, 1999), and preferentially select diets of 15% protein (Lewis et al., 2001), indicating that our observed trophic discrimination in some EAAs could indeed be the result of catabolism and oxidation of surplus EAAs. The assimilation of EAAs from gut microbes can also impact trophic discrimination, though this is particularly prevalent in low-protein diets (e.g. <10% crude protein; Newsome et al., 2020). Furthermore, we would expect gut microbial EAAs to skew $\delta^{13}C$ fingerprints towards bacteria, but this was not the case, indicating that microbial endosymbionts likely did not impact our results. However, despite these presumed physiological effects, trophic fractionation did not fundamentally alter $\delta^{13}C$ fingerprints or dietary assignment of consumer tissues. Indeed, all individuals from single protein treatments classified perfectly with their respective diets (Figure 2b,c). These results indicate that the assumption of perfect routing of $\delta^{13}C$ fingerprints from dietary protein to consumer tissues was not explicitly violated; nevertheless, trophic fractionation does occur, and future research should consider the potential effects of dietary protein content on trophic discrimination and $\delta^{13}C$ fingerprints.

We used a series of isotopic mixing models and an LDA bootstrapping approach to estimate the proportional contributions of protein sources to consumer diets, but some departures from known diets were present. Most notably, all approaches overestimated the contribution of plant-based protein to mice in the mixed protein treatment (Figure 3). We hypothesize that this result was physiological rather than methodological, and most likely a consequence of digestive efficiency. Our experiment used soy protein, torula yeast and a methanotrophic single-celled bacterial protein meal (FeedKind®) as our plant, fungal and bacterial protein sources, respectively. Previous faecal and ileal analyses from feeding experiments have shown that the apparent digestibility of EAAs in soy protein is higher than that of yeast or bacterial protein in multiple species (e.g. mice [*Mus musculus*], pigs [*Sus domesticus*], mink [*Mustela vison*] and chickens [*Gallus gallus domesticus*]; Keith & Bell, 1988, Skrede et al., 1998, Schøyen et al., 2007, Moehn et al., 2010, Wang et al., 2013, Park et al., 2021). For example, the six EAAs measured in this experiment are on average 8.9% more digestible in soy than in yeast (Park et al., 2021), and 3.75% more digestible in soy compared to bacterial protein (Schøyen et al., 2007; Wang et al., 2013). Furthermore, the three most informative EAAs for $\delta^{13}C$ fingerprinting (Leu, Ile, Lys) are 3.6%–7.0% more digestible in soy than in bacterial and fungal proteins (Park et al., 2021; Schøyen et al., 2007; Wang et al., 2013). Thus, it is likely that the observed overrepresentation of plant protein in the mixed diet treatment in both our LDA and proportional diet estimates was due in part to higher digestibility and assimilation of soy derived EAAs. Similarly, the biological value of protein sources—here defined as the degree to which the amino acid profile of the diet matches the amino acid profile of the consumer—could have influenced EAA assimilation and $\delta^{13}C$ fingerprints. For example, the relative proportion of Leu, the most influential EAA in our LDA, was highest in soy protein and most closely matched the proportions in mouse liver and muscle tissue (Figure S4). Assuming mice assimilated EAAs in proportion to their relative availability, it is likely that both digestibility and biological value contributed to the consistent overrepresentation of plant-based protein in proportional diet estimates.

All models accurately estimated source contributions for single protein diet treatments, but mixing model-based approaches consistently performed best across diet treatments. Furthermore, we tested the application of EAA-specific TDFs ($\Delta^{13}C_{Tissue\text{-}Diet}$) to our mixing models and found that models with and without TDFs performed comparably, with nearly identical proportional diet estimates for most treatments (Figure S2, Appendix 2). Given the previously noted uncertainty in trophic fractionation of EAAs, this result provides flexibility for future researchers. Similarly, many studies do not have access to measured EAA $\delta^{13}C$ values from local sources and instead use previously published data from potential sources. We found that the use of published $\delta^{13}C$ fingerprints for the plant, bacterial and fungal sources (e.g. Larsen et al., 2009, 2013) can lead to erroneous classifications (Figure 4), and we strongly caution against the widespread application of such data to estimate multichannel feeding. Instead, we encourage researchers to apply local or regional $\delta^{13}C$ fingerprints, and, when possible, to generate EAA $\delta^{13}C$ values for their potential sources directly. Nevertheless, even regional fingerprint data could cause similar problems as baseline $\delta^{13}C$ values can vary significantly at fine spatial scales. In such instances, we do not recommend using measured EAA $\delta^{13}C$ values themselves. Rather, our results suggest that researchers can use LDA coordinates from regional sources as end members in Bayesian mixing models to estimate proportional diet contributions, given that source fingerprints are more likely to be conserved than measured EAA $\delta^{13}C$ values (this study; Larsen et al., 2009, 2013). Lastly, our analyses corroborated previous studies and found almost no effect of data normalization (Fox et al., 2019; Larsen et al., 2015). Collectively, these results provide flexibility for researchers looking to employ $\delta^{13}C$ fingerprinting in the absence of site-specific data.

Like many isotope-based approaches for estimating dietary proportions, the geometry of the isotopic mixing space must be considered when applying either LDA or Bayesian mixing models. For example, we found that LDA bootstrapping assigned all mixed diet animals to the plant protein treatment, resulting in extreme deviations from the known dietary proportions (Figure 3). This was likely because all source measurements used in our experiment were pseudoreplicates of three dietary proteins (soy, torula yeast and FeedKind®), thereby limiting $\delta^{13}C$ variation within treatments while LDA maximized variation between treatments. Consequently, iterative resampling had minimal impact on the overall LDA space, leading to limited variation in source error distributions and the classification of consumer tissues. Future research employing such approaches should consider the relative spacing and variability in $\delta^{13}C$ fingerprints, particularly when LDA reveals substantial differences between sources. Similarly, our mixing models were likely affected by the isotopic variation in source proteins. For instance, $\delta^{13}C$ EAA values in soy (~ −25‰), torula yeast (~ −10‰) and bacterial protein (~ −40‰) were evenly separated by ~15‰ (Figure S5). Such isotopic separation is rare in wild systems and could have artificially increased the precision of our mixing models. Likewise, these patterns created linearity in our mixing space, resulting in greater uncertainty for the 'central' source, plants, compared to bacteria and fungi (Figure 3; Figure S5). Nevertheless, this error was reduced when applying all six EAAs, suggesting that more isotopic tracers increase the accuracy of dietary estimates.

### 4.1 | Future directions and recommendations

We have shown that $\delta^{13}C$ fingerprinting is a powerful tool for quantifying energy flow and multichannel feeding, but important considerations remain. For example, we observed significant trophic fractionation in EAA $\delta^{13}C$ values and therefore encourage additional feeding experiments to assess the consistency of $\delta^{13}C$ fingerprint assimilation by consumers. It is likely that protein content and quality, in particular, affect trophic fractionation in EAAs (Whiteman et al., 2021), and we suggest future experiments use more natural diet treatments with digestibility, biological values and isotopic compositions more comparable to wild systems (sensu Pollierer

et al., 2019). Furthermore, we tested the assimilation of $\delta^{13}C$ fingerprints from plant, fungal and bacterial proteins, but algae and other marine producers also exhibit unique $\delta^{13}C$ fingerprints (Elliott Smith et al., 2020; Larsen et al., 2013), and the assimilation of these source fingerprints by consumers remains uncertain (Larsen et al., 2013; McMahon et al., 2015). To that end, we encourage researchers to collect and analyse site-specific source data, as we found the use of published fingerprints may lead to erroneous estimates of multichannelling when applied across systems. This is likely because many published $\delta^{13}C$ fingerprints were derived from cultured sources where all EAA were synthesized de novo in the absence of organic nitrogen (e.g. Larsen et al., 2009). However, wild sources like plants and fungi often exchange amino acids (Hobbie & Hobbie, 2006) or uptake free amino acids in soil (Näsholm et al., 2009), potentially altering source $\delta^{13}C$ fingerprints across space and time. Consequently, the application of $\delta^{13}C$ fingerprinting to wild consumers will be contingent upon understanding EAA exchange not only from source to consumer, but also among potential sources of EAAs.

We conducted the first empirical tests of proportional diet estimation using $\delta^{13}C$ fingerprinting, and our results provide a blueprint for future research. For specialized consumers using single energy channels, we show that either Bayesian mixing models or LDA bootstrapping can accurately estimate diet proportions, while mixing models provide more accuracy when trying to estimate the use of multiple energy channels. Importantly, we show that mixing models can be parameterized directly with EAA $\delta^{13}C$ values or with LDA coordinates, and that these models can accurately estimate dietary proportions with or without the use of TDFs. However, we recommend that researchers use EAA $\delta^{13}C$ values and TDFs when available, as these models provided the most accurate estimates of proportional diets in our experiment. Furthermore, we recommend researchers measure and employ as many EAAs as possible, as the full suite of measured EAAs provided more accurate and less variable diet estimates compared to a subset of EAAs. We also note that, as with all mixing models, accurate estimates of dietary proportions still require isotopic separation among sources and low linearity in the mixing space (Phillips et al., 2014). Collectively, we believe these best practices will allow researchers to accurately estimate multichannel feeding and food web connectivity, but future feeding studies should continue to test and refine approaches for estimating proportional contributions of energy channels to consumer diets.

## AUTHORS' CONTRIBUTIONS

Both authors conceived of the study and designed the experiment; P.J.M. collected and analysed the data. Both authors contributed to writing and gave final approval for publication.

## ACKNOWLEDGEMENTS

We thank C. Mancuso, S. Farr, A. Martinez and J. Sharp for animal husbandry support; UNM-ARF for in-kind support; and N. Lübcker, C. Mancuso and O. Shipley for comments on the manuscript. Research was supported by an NSF Division of Integrative Organismal Systems grant (IOS-1755402) to SDN and PJM was supported by an NSF Postdoctoral Research Fellowship (DBI-2010712).

## CONFLICT OF INTEREST

The authors declare no conflict of interest.

## PEER REVIEW

The peer review history for this article is available at https://publons.com/publon/10.1111/2041-210X.13903.

## DATA AVAILABILITY STATEMENT

All data and R scripts available at https://doi.org/10.6084/m9.figshare.17298980.v1 (Manlick & Newsome, 2022).

## ORCID

*Philip J. Manlick* https://orcid.org/0000-0001-9143-9446
*Seth D. Newsome* https://orcid.org/0000-0002-4534-1242

## REFERENCES

Arthur, K. E., Kelez, S., Larsen, T., Choy, C. A., & Popp, B. N. (2014). Tracing the biosynthetic source of essential amino acids in marine turtles using $\delta^{13}C$ fingerprints. *Ecology*, *95*, 1285–1293.

Butler, J. L., Gotelli, N. J., & Ellison, A. M. (2008). Linking the brown and green: Nutrient transformation and fate in the Sarracenia microecosystem. *Ecology*, *89*, 898–904.

Dalerum, F., & Angerbjörn, A. (2005). Resolving temporal variation in vertebrate diets using naturally occurring stable isotopes. *Oecologia*, *144*, 647–658.

Elliott Smith, E. A., Harrod, C., Docmac, F., & Newsome, S. D. (2020). Intraspecific variation and energy channel coupling within a Chilean kelp forest. *Ecology*, *102*, 1–13.

Fox, M. D., Elliot Smith, E. A., Smith, J. E., & Newsome, S. D. (2019). Trophic plasticity in a common reef-building coral: Insights from $\delta^{13}C$ analysis of essential amino acids (accepted). *Functional Ecology*, *33*, 1–12.

Harada, Y., Lee, S., Connolly, R., & Fry, B. (2022). Compound-specific isotope analysis of amino acids reveals dependency on grazing rather than detritivory in mangrove food webs. *Marine Ecology Progress Series*, *681*, 13–20.

Hobbie, J. E., & Hobbie, E. A. (2006). $^{15}N$ in symbiotic fungi and plants estimates nitrogen and carbon flux rates in arctic tundra. *Ecology*, *87*, 816–822.

Keith, M. O., & Bell, J. M. (1988). Digestibility of nitrogen and amino acids in selected protein sources fed to mice. *Journal of Nutrition*, *118*, 561–568.

Larsen, T., Bach, L. T., Salvatteci, R., Wang, Y. V., Andersen, N., Ventura, M., & McCarthy, M. D. (2015). Assessing the potential of amino acid $^{13}C$ patterns as a carbon source tracer in marine sediments: Effects of algal growth conditions and sedimentary diagenesis. *Biogeosciences*, *12*, 4979–4992.

Larsen, T., Taylor, D., Leigh, M., & O'Brien, D. (2009). Stable isotope fingerprinting: A novel method for identifying plant, fungal, or bacterial origins of amino acids. *Ecology*, *90*, 3526–3535.

Larsen, T., Ventura, M., Andersen, N., O'Brien, D. M., Piatkowski, U., & McCarthy, M. D. (2013). Tracing carbon sources through aquatic and terrestrial food webs using amino acid stable isotope fingerprinting. *PLoS ONE*, *8*, e73441.

Lewis, C. E., Clark, T. W., & Derting, T. L. (2001). Food selection by the white-footed mouse (*Peromyscus leucopus*) on the basis of energy and protein contents. *Canadian Journal of Zoology*, *79*, 562–568.

Lindeman, R. L. (1942). The trophic-dynamic aspect of ecology. *Ecology*, *23*, 399–417.

Manlick, P. J., & Newsome, S. D. (2022). Data from: Stable isotope fingerprinting traces essential amino acid assimilation and multichannel feeding in a vertebrate consumer. *Figshare*, https://doi.org/10.6084/m9.figshare.17298980.

McAdam, A. G., & Millar, J. S. (1999). The effects of dietary protein content on growth and maturation in deer mice. *Canadian Journal of Zoology*, *77*, 1822–1828.

McMahon, K. W., Fogel, M. L., Elsdon, T. S., & Thorrold, S. R. (2010). Carbon isotope fractionation of amino acids in fish muscle reflects biosynthesis and isotopic routing from dietary protein. *Journal of Animal Ecology*, *79*, 1132–1141.

McMahon, K. W., Polito, M. J., Abel, S., Mccarthy, M. D., & Thorrold, S. R. (2015). Carbon and nitrogen isotope fractionation of amino acids in an avian marine predator, the gentoo penguin (*Pygoscelis papua*). *Ecology and Evolution*, *5*, 1278–1290.

McMahon, K. W., Thorrold, S. R., Houghton, L. A., & Berumen, M. L. (2016). Tracing carbon flow through coral reef food webs using a compound-specific stable isotope approach. *Oecologia*, *180*, 809–821.

Miller, J. F., Millar, J. S., & Longstaffe, F. J. (2008). Carbon- and nitrogen-isotope tissue-diet discrimination and turnover rates in deer mice, *Peromyscus maniculatus*. *Canadian Journal of Zoology*, *86*, 685–691.

Moehn, S., Groenewegen, P., & Ball, R. O. (2010). Amino acid digestibility of a yeast-derived protein source and gut endogenous losses in newly weaned pigs. *Livestock Science*, *134*, 221–224.

Näsholm, T., Kielland, K., & Ganeteg, U. (2009). Uptake of organic nitrogen by plants. *New Phytologist*, *182*, 31–48.

Newsome, S. D., Feeser, K. L., Bradley, C. J., Wolf, C., Takacs-Vesbach, C., & Fogel, M. L. (2020). Isotopic and genetic methods reveal the role of the gut microbiome in mammalian host essential amino acid metabolism. *Proceedings of the Royal Society B*, *287*(1922), 20192995.

Noble, J. D., Collins, S. L., Hallmark, A. J., Maldonado, K., Wolf, B. O., & Newsome, S. D. (2019). Foraging strategies of individual silky pocket mice over a boom–bust cycle in a stochastic dryland ecosystem. *Oecologia*, *190*, 569–578.

O'Brien, D. M., Fogel, M. L., & Boggs, C. L. (2002). Renewable and nonrenewable resources: Amino acid turnover and allocation to reproduction in lepidoptera. *Proceedings of the National Academy of Sciences of the United States of America*, *99*, 4413–4418.

Oksanen, J., Blanchet, F. G., Kindt, R., Legendre, P., Minchin, P. R., O'hara, R. B., Simpson, G. L., Solymos, P., Stevens, M. H. H., Wagner, H., & Oksanen, M. J. (2013). *Package 'vegan'*. Community ecology package, version 2.9.

Park, C. S., Aderibigbe, A. S., Ragland, D., & Adeola, O. (2021). Digestible and metabolizable energy concentrations and amino acid digestibility of dried yeast and soybean meal for growing pigs. *Journal of Animal Science*, *99*, 1–10.

Parnell, A. C., & Inger, R. (2016). *Simmr: A stable isotope mixing model*. Statistical package in R Software. R package version 0.3.

Pauli, J. N., Manlick, P. J., Dharampal, P. S., Takizawa, Y., Chikaraishi, Y., Niccolai, L. J., Grauer, J. A., Black, K. L., Garces Restrepo, M., Perrig, P. L., Wilson, E. C., Martin, M. E., Rodriguez Curras, M., Bougie, T. A., Thompson, K. L., Smith, M. M., & Steffan, S. A. (2019). Quantifying niche partitioning and multichannel feeding among tree squirrels. *Food Webs*, *21*, e00124.

Perkins, M. J., Inger, R., Bearhop, S., & Sanders, D. (2017). Multichannel feeding by spider functional groups is driven by feeding strategies and resource availability. *Oikos*, *127*, 23–33.

Phillips, D. L., Inger, R., Bearhop, S., Jackson, A. L., Moore, J. W., Parnell, A. C., Semmens, B. X., & Ward, E. J. (2014). Best practices for use of stable isotope mixing models in food web studies. *Canadian Journal of Zoology*, *835*, 823–835.

Polis, G. A. (1991). Complex trophic interactions in deserts: An empirical critique of food-web theory. *The American Naturalist*, *138*, 123–155.

Polis, G. A., & Strong, D. R. (1996). Food web complexity and community dynamics. *The American Naturalist*, *147*, 813–846.

Pollierer, M. M., Larsen, T., Potapov, A., Brückner, A., Heethoff, M., Dyckmans, J., & Scheu, S. (2019). Compound-specific isotope analysis of amino acids as a new tool to uncover trophic chains in soil food webs. *Ecological Monographs*, *89*, 1–24.

Potapov, A. M., Tiunov, A. V., & Scheu, S. (2019). Uncovering trophic positions and food resources of soil animals using bulk natural stable isotope composition. *Biological Reviews*, *94*, 37–59.

Potapov, A. M., Tiunov, A. V., Scheu, S., Larsen, T., & Pollierer, M. M. (2019). *Combining bulk and amino acid stable isotope analyses to quantify trophic level and basal resources of detritivores: A case study on earthworms. Oecologia*. Springer Berlin Heidelberg.

Ripley, B., Venables, B., Bates, D. M., Hornik, K., Gebhardt, A., Firth, D., & Ripley, M. B. (2013). Package 'mass' Cran r, *538*, 113–120.

Schøyen, H. F., Hetland, H., Rouvinen-Watt, K., & Skrede, A. (2007). Growth performance and ileal and total tract amino acid digestibility in broiler chickens fed diets containing bacterial protein produced on natural gas. *Poultry Science*, *86*, 87–93.

Sikes, R. S. (2016). 2016 guidelines of the American Society of Mammalogists for the use of wild mammals in research and education. *Journal of Mammalogy*, *97*, 663–688.

Silfer, J. A., Engel, M. H., Macko, S. A., & Jumeau, E. J. (1991). Stable carbon isotope analysis of amino acid enantiomers by conventional isotope ratio mass spectrometry and combined gas chromatography/isotope ratio mass spectrometry. *Analytical Chemistry*, *63*, 370–374.

Skrede, A., Berge, G. M., Storebakken, T., Herstad, O., Aarstad, K. G., & Sundstøl, F. (1998). Digestibility of bacterial protein grown on natural gas in mink, pigs, chicken and Atlantic salmon. *Animal Feed Science and Technology*, *76*, 103–116.

Steffan, S. A., Chikaraishi, Y., Dharampal, P. S., Pauli, J. N., Guédot, C., & Ohkouchi, N. (2017). Unpacking brown food-webs: Animal trophic identity reflects rampant microbivory. *Ecology and Evolution*, *7*, 3532–3541.

Symondson, W. O. C. (2002). Molecular identification of prey in predator diets. *Molecular Ecology*, *11*, 627–641.

Thompson, R. M., Brose, U., Dunne, J. A., Hall, R. O., Hladyz, S., Kitching, R. L., Martinez, N. D., Rantala, H., Romanuk, T. N., Stouffer, D. B., & Tylianakis, J. M. (2012). Food webs: Reconciling the structure and function of biodiversity. *Trends in Ecology & Evolution*, *27*, 689–697.

Thorp, J. H., & Bowes, R. E. (2017). Carbon sources in riverine food webs: New evidence from amino acid isotope techniques. *Ecosystems*, *20*, 1029–1041.

Vander Zanden, M. J., & Vadeboncoeur, Y. (2002). Fishes as integrators of benthic and pelagic food webs in lakes. *Ecology*, *83*, 2152–2161.

Wang, J. P., Kim, J. D., Kim, J. E., & Kim, I. H. (2013). Amino acid digestibility of single cell protein from Corynebacterium ammoniagenes in growing pigs. *Animal Feed Science and Technology*, *180*, 111–114.

Whiteman, J. P., Elliott Smith, E., Besser, A., & Newsome, S. (2019). A guide to using compound-specific stable isotope analysis to study the fates of molecules in organisms and ecosystems. *Diversity*, *11*, 8.

Whiteman, J. P., Kim, S. L., McMahon, K. W., Koch, P. L., & Newsome, S. D. (2018). Amino acid isotope discrimination factors for a carnivore: Physiological insights from leopard sharks and their diet. *Oecologia*, *188*, 977–989.

Whiteman, J. P., Rodriguez Curras, M., Feeser, K. L., & Newsome, S. D. (2021). Dietary protein content and digestibility influences discrimination of amino acid nitrogen isotope values in a terrestrial omnivorous mammal. *Rapid Communications in Mass Spectrometry*, *35*, e9073.

Wolf, N., Newsome, S. D., Peters, J., & Fogel, M. L. (2015). Variability in the routing of dietary proteins and lipids to consumer tissues influences tissue-specific isotopic discrimination. *Rapid Communications in Mass Spectrometry*, *29*, 1448–1456.

Wolkovich, E. M., Allesina, S., Cottingham, K. L., Moore, J. C., Sandin, S. A., & De Mazancourt, C. (2014). Linking the green and brown worlds: The prevalence and effect of multichannel feeding in food webs. *Ecology*, *95*, 3376–3386.

Wu, G. (1998). Intestinal mucosal amino acid catabolism. *Journal of Nutrition*, *128*, 1249–1252.

Wu, G. (2009). Amino acids: Metabolism, functions, and nutrition. *Amino Acids*, *37*, 1–17.

Zou, K., Thébault, E., Lacroix, G., & Barot, S. (2016). Interactions between the green and brown food web determine ecosystem functioning. *Functional Ecology*, *30*, 1454–1465.

## SUPPORTING INFORMATION

Additional supporting information may be found in the online version of the article at the publisher's website.

**How to cite this article:** Manlick, P. J., & Newsome, S. D. (2022). Stable isotope fingerprinting traces essential amino acid assimilation and multichannel feeding in a vertebrate consumer. *Methods in Ecology and Evolution*, *00*, 1–12. https://doi.org/10.1111/2041-210X.13903